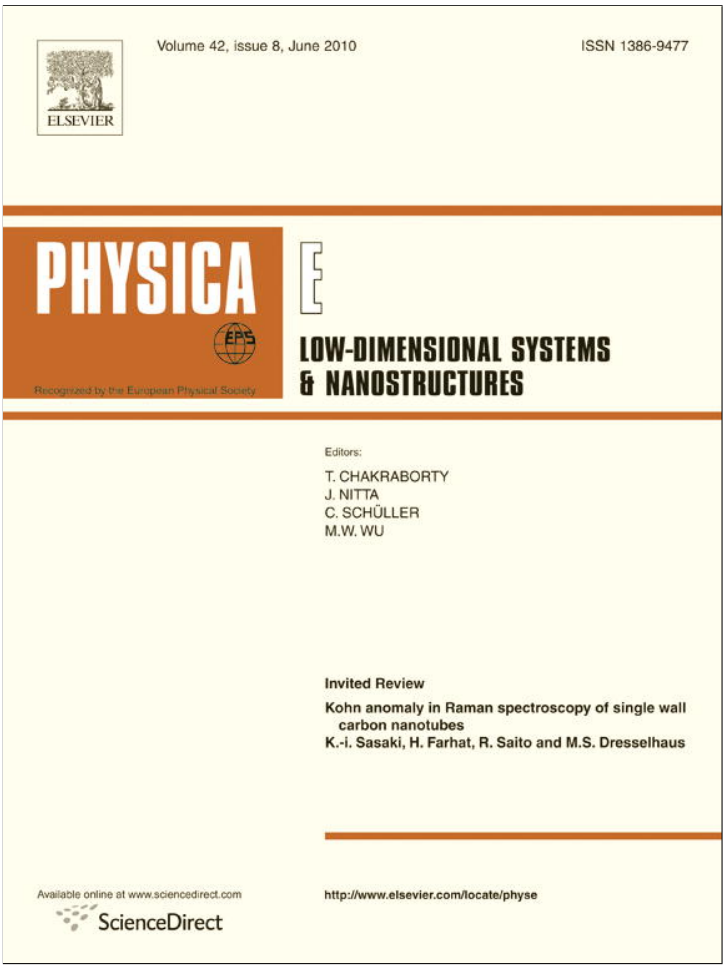

Physica E 42 (2010) 2036–2040

Contents lists available at ScienceDirect

Physica E

journal homepage: www.elsevier.com/locate/physe

Elasticity and piezoelectricity of zinc oxide nanostructure

R. Chowdhury [a,*], S. Adhikari [a], F. Scarpa [b]

[a] Multidisciplinary Nanotechnology Centre, Swansea University, Singleton Park, Swansea SA2 8PP, UK
[b] Advanced Composites Centre for Innovation and Science, University of Bristol, Bristol BS8 1TR, UK

ARTICLE INFO

Article history:
Received 8 January 2010
Accepted 16 March 2010
Available online 19 March 2010

Keywords:
ZnO nanotube
Elasticity
Piezoelectricity
Molecular simulation

ABSTRACT

ZnO nanotubes have the potential to be used widely in variety of nano electromechanical devices. We calculate the elastic and piezoelectric properties of single wall ZnO nanotubes using molecular simulations. A Buckingham type interatomic potential has been used for numerical calculations. Prior to estimate the properties of tubular system, we have calculated the ZnO crystal of wurtzite structure and validated our results with other available results. The results are in good agreement with literature, using present computational approach. Finally, we studied the properties of ZnO nanotubes. Our results indicate that the elastic properties (e.g., the elements of the elastic tensor) of ZnO nanotubes decrease with the increase in tube diameter. The piezoelectric property of ZnO NTs is also found to be dependent on the tube diameter.

1. Introduction

Zinc oxide (ZnO) [1] materials have attracted extensive attention due of their excellent performance in electronic, ferroelectric, piezoelectric [2,3] and optical applications [4,5]. With a band gap in the ($\sim$3.37 eV) range [6,7] and a large exciton binding energy ($\sim$60 meV) at room temperature, ZnO [8] has many potential advantages in ultraviolet optoelectronic devices. It can be used in the fields of blue and ultraviolet lasers, light-emitting diodes, and solar cells [9,4,10]. Nano-scale ZnO is also an important material [11,12] for the nanoscale energy harvesting and scavenging [13–16]. In recent years, a great variety of ZnO nanostructures [11,17,18] are being synthesized [17,19], and the structural [20,21], mechanical [22,23], optical and electrical [24,25] properties are investigated experimentally [26,27]. With regards to the mechanical properties [28,29], it is found that the bending moduli of ZnO nanobelts are dependent on the aspect ratio in the growth direction [30,31], whereas it is independent on their surface-to-volume ratio [23]. For ZnO nanowires, it is found that the Young's moduli [32] increased as the diameter decreased, and the values of these Young's moduli were all larger than the bulk value. On the theoretical side, the surface stress induced internal compressive stress played an important role in the change of the Young's modulus [33,34]. Investigation and understanding of the mechanical as well piezoelectric properties of ZnO nanostructure are valuable for their potential application. For example, ZnO nanotubes are bend by rubbing against each other for energy scavenging [13–16]. In this study, we present the results of elastic tensors and piezoelectric coefficients of ZnO crystals as well ZnO nanotubes grown from wurtzite crystal and arrive at nanotube structure. We also compare our results with the experimental results and previous theoretical results available in the literature.

2. The computational approach

A Buckingham type interatomic potential [35]

$$U(r_{ij}) = \frac{q_i q_j}{r_{ij}} + A\exp\left(-\frac{r_{ij}}{\rho}\right) - \frac{C}{r_{ij}^6} \quad (1)$$

is used in this study. Here U is the pair potential energy contributed by the interaction between the ith and jth ions with a distance of r_{ij}, q_i is the charge of the ith ion and the parameters of A, ρ and C for ZnO are given in [33]. The first term in Eq. (1) describes the long-range Coulomb interactions between two ions, and the second and the third terms represent their short-range interactions. To handle the long-range Coulomb interactions, we utilize the corrected Ewald summation [36,37] to reduce the computational demand as well as to enhance the computational efficiency.

Using the optimized structure, we can calculate the elements of the elastic tensor and piezoelectric coefficients. The elements of the elastic tensor reflect the stress–strain relation of materials. In terms of the symmetry of ZnO, this relation can be expressed in

* Corresponding author. Tel.: +44 1792 602088; fax: +44 1792 295676.
E-mail addresses: R.Chowdhury@swansea.ac.uk, crajib2003@gmail.com (R. Chowdhury), S.Adhikari@swansea.ac.uk (S. Adhikari), f.scarpa@bris.ac.uk (F. Scarpa).

1386-9477/$ - see front matter © 2010 Elsevier B.V. All rights reserved.
doi:10.1016/j.physe.2010.03.018

the matrix form

$$\begin{pmatrix}\sigma_1\\ \sigma_2\\ \sigma_3\\ \sigma_4\\ \sigma_5\\ \sigma_6\end{pmatrix}=\begin{pmatrix}c_{11} & c_{12} & c_{13} & 0 & 0 & 0\\ c_{12} & c_{11} & c_{13} & 0 & 0 & 0\\ c_{13} & c_{13} & c_{33} & 0 & 0 & 0\\ 0 & 0 & 0 & c_{44} & 0 & 0\\ 0 & 0 & 0 & 0 & c_{44} & 0\\ 0 & 0 & 0 & 0 & 0 & (c_{11}-c_{12})/2\end{pmatrix}\begin{pmatrix}\varepsilon_1\\ \varepsilon_2\\ \varepsilon_3\\ \varepsilon_4\\ \varepsilon_5\\ \varepsilon_6\end{pmatrix} \quad (2)$$

where σ_i and ε_i ($i=1,\ldots,6$) represent the stresses and strains, respectively. Similarly, the piezoelectricity can be expressed (ref (3)) in the matrix form [2,3,38] as

$$\begin{pmatrix}P_1\\ P_2\\ P_3-P_3^0\end{pmatrix}=\begin{pmatrix}0 & 0 & 0 & 0 & e_{15} & 0\\ 0 & 0 & 0 & e_{15} & 0 & 0\\ e_{31} & e_{31} & e_{33} & 0 & 0 & 0\end{pmatrix}\begin{pmatrix}\varepsilon_1\\ \varepsilon_2\\ \varepsilon_3\\ \varepsilon_4\\ \varepsilon_5\\ \varepsilon_6\end{pmatrix} \quad (3)$$

where P_1, P_3, and P_2 are three polarization components along the a direction, the c direction, the direction perpendicular to a and c, respectively. P_3^0 is the spontaneous polarization along the c direction. There are only three independent piezoelectric coefficients: e_{31}, e_{33}, and e_{15}.

The elastic tensor of a system can be represented by elastic constants (C_{ij}, (i, $j=1,\ldots,6$)), Young's modulus (E_i, ($i=1,2,3$)), bulk (K) and shear (G) modulus, Poisson's ratio (v). The elastic constants represent the second derivatives of the energy density with respect to strain:

$$C_{ij}=\frac{1}{V}\left(\frac{\partial^2 U}{\partial\varepsilon_i\partial\varepsilon_j}\right) \quad (4)$$

thereby describing the mechanical hardness of the material with respect to deformation. Since there are 6 possible strains within the notation scheme employed here, the elastic constant tensor is a 6×6 symmetric matrix. However, in ZnO-like symmetry system, there are only five independent constants (C_{11}, C_{12}, C_{13}, C_{33}, C_{44}). In calculating the second derivatives of the energy with respect to strain, it is important to allow for the response of all internal degrees of freedom of the crystal to the perturbation. If the following notation for the second-derivative matrices is introduced:

$$D_{\varepsilon\varepsilon}=\left(\frac{\partial^2 U}{\partial\varepsilon\partial\varepsilon}\right)_{internal},\quad D_{\varepsilon i}=\left(\frac{\partial^2 U}{\partial\varepsilon\partial\alpha_i}\right)_{\varepsilon},\quad D_{ij}=\left(\frac{\partial^2 U}{\partial\alpha_i\partial\beta_j}\right)_{\varepsilon} \quad (5)$$

then the full expression for the elastic constant tensor can be written as [39]

$$C_{ij}=\frac{1}{V}(D_{\varepsilon\varepsilon}-D_{\varepsilon i}D_{ij}^{-1}D_{j\varepsilon}) \quad (6)$$

The elastic compliances, S, can be readily calculated from the above expression by inverting the matrix (i.e. $S=C^{-1}$). Like the elastic constant tensor, the bulk (K) and shear (G) moduli contain information regarding the hardness of a material with respect to various types of deformation. Experimentally a bulk modulus is much more facile to determine than the elastic constant tensor. If the structure of a material is studied as a function of applied isotropic pressure, then a plot of pressure versus volume can be fitted to an equation of state where the bulk modulus is one of the curve parameters. Typically a third or fourth order Birch–Murgnahan equation of state is utilized [40]. The bulk and shear moduli are clearly related to the elements of the elastic constant. However, there is no unique definition of this transformation [40]. In this study, we calculated bulk and shear moduli definitions due to Voight [38,41]. Below are the equations for the Voight definition [40,41]:

$$K_{Voight}=\tfrac{1}{9}(C_{11}+C_{22}+C_{33}+2(C_{12}+C_{13}+C_{23}))$$

$$G_{Voight}=\tfrac{1}{15}(C_{11}+C_{22}+C_{33}+3(C_{44}+C_{55}+C_{66})-C_{12}-C_{13}-C_{23}) \quad (7)$$

When an uniaxial tension is applied to a material then the lengthening of the material is measured according to the strain. The ratio of stress to strain defines the value of the Young's modulus for that axis $E_\alpha=\sigma_{\alpha\alpha}/\varepsilon_{\alpha\alpha}$. Since a thermodynamically correct material will always increase in length under tension, the value of this quantity should always be positive. The Young's moduli in each of the Cartesian directions can be calculated from the elastic compliances as $E_x=S_{11}^{-1}$, $E_y=S_{22}^{-1}$ and $E_z=S_{33}^{-1}$. Complementary to Young's modulus is the Poisson ratio, which measures the change in a material at right angles to the uniaxial stress. Formally it is defined as the ratio of lateral to longitudinal strain under a uniform, uniaxial stress. The expression used to calculate this property, assuming an isotropic medium, is given below [38]:

$$\sigma_\alpha(\beta)=-S_{\alpha\alpha\beta\beta}E_\beta \quad (8)$$

Because most materials naturally shrink orthogonal to an applied tension this leads to positive values for Poisson's ratio, with a theoretical maximum of 0.5. Typical values for many materials lie in the range 0.2–0.3, though negative values are also known. For an isotropic material this quantity can also be related to the bulk modulus as [40,41] $K=(1/3)E/(1-2\sigma)$.

The piezoelectric constants are key quantities in many technological applications such as energy scavenging [13–16], since they govern the correlation between the strain and applied electric field for non-centrosymmetric materials (centrosymmetric materials necessarily have zero for all piezoelectric constants). In this study, the piezoelectric strain constants, e, are calculated as [40]

$$e_{\alpha i}=\frac{\partial P_\alpha}{\partial\varepsilon_i} \quad (9)$$

The above piezoelectric strain constants can be readily transformed into piezoelectric stress constants by the multiplication with the elastic compliance tensor.

3. Properties of ZnO crystal and validation of the results

The ground state of a ZnO crystal has a wurtzite structure (polar hexagonal space group $P\,63mc$) two formula-units with two zinc and two oxygen atoms per unit cell as shown in Fig. 1. The lattice constants and internal parameter obtained from experiments are as follows: $a=b=3.250$ Å, $c=5.204$ Å, and $u=0.382$, respectively [3]. Using the potential model adopted in this study, the optimal lattice constants of wurtzite ZnO are

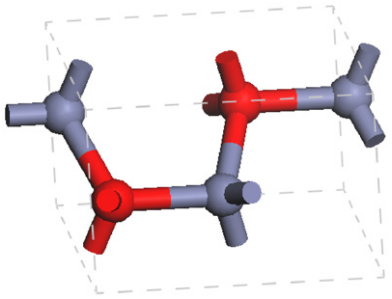

Fig. 1. Unit cell of wurtzite ZnO. Red and light gray colour represents Oxygen and Zinc atoms, respectively. (For interpretation of the references to colour in this figure legend, the reader is referred to the web version of this article.)

Table 1
Comparison of the optimized results of the ZnO with other results.

	a (Å)	c (Å)	c/a
Computed value	3.268	5.192	1.588
DFPT [2]	3.199	5.167	1.615
DFT [43]	3.197	5.166	1.616
Hartree-Fock [42]	3.286	5.241	1.595
Experiment [3]	3.250	5.204	1.602
Experiment [44]	3.250	5.207	1.602
Error (%)	0.55	0.29	0.87

Table 2
Elastic constants relaxed state of ZnO crystals in units of GPa.

	c_{11}	c_{12}	c_{13}	c_{44}	c_{33}
Computed value	184	93	77	56	206
DFPT [2]	218	137	121	38	229
DFT [43]	226	139	123	40	242
Hartree–Fock [42]	246	127	105	56	246
DFT [21]	246	127	104	56	242
Experiment [45]	207	118	106	45	210
Experiment [46]	190	110	90	39	196

Table 3
Piezoelectric strain matrix of ZnO crystals in units of C/m^2.

	e_{31}	e_{33}	e_{15}
Computed value	−0.74	1.01	−0.44
DFPT [2]	−0.65	1.24	−0.54
DFT [43]	−0.67	1.28	−0.53
Hartree–Fock [42]	−0.55	1.19	−0.46
Experiment [45]	−0.62	0.96	−0.37

evaluated and compared with other results [2,3,42,43]. It is easy to see from Table 1 that our results are quite close to those of other theoretical results and agree well with the experimental results [44] (errors are around 1%). Using the optimized structure of wurtzite ZnO, we can calculate the elements of the elastic tensor and piezoelectric coefficients. The values of elastic constants computed in the present work are listed in Table 2 along with other reference works.

Note that for c_{66} a value of about 45 GPa is obtained by using $c_{66}=1/2(c_{11}-c_{12})$ as must hold for hexagonal systems. Similarly, the piezoelectric coefficients (ref Eq. (3)) computed in the present work are listed in Table 3 along with other reference works.

Good agreements have been achieved between the present results and those in the literature (presented in Tables 2 and 3). Confirming that our computational procedure can give reasonable results for bulk ZnO systems, we proceed to analyze ZnO single wall nanotubes.

4. Simulation details for ZnO nanotubes

Recently, ZnO nanostructures, specifically nanowires and nanobelts, have been extensively studied because of their potential applications. In contrast, limited works on ZnO nanotubes are reported [47]. Particularly, it seems hard to obtain the tubular structure of the ZnO material as no layered ZnO exists [47]. The hollow 1D ZnO structure could provide more prominent advantages than other 1D ZnO materials like nanowires and nanobelts. Several groups have synthesized hexagonal ZnO nanotubes [48,49], though single-walled ZnO nanotubes with a round wall have not been realized. A recent study [2] indicated

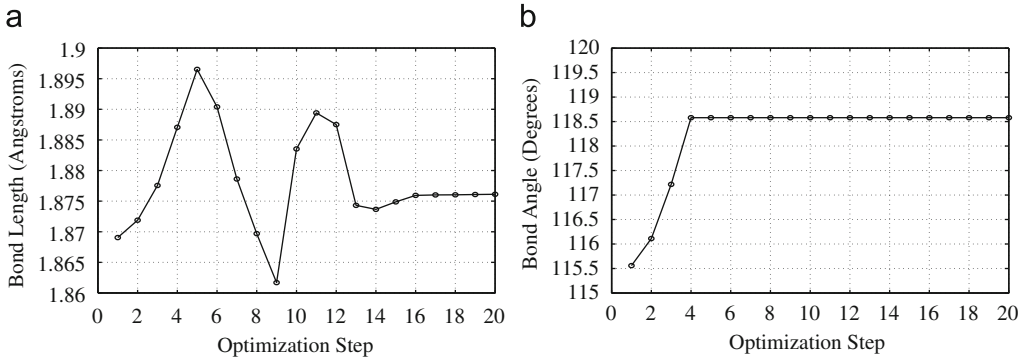

Fig. 2. The optimization of the bond properties of a typical ZnO nanotube. (a) The optimization of bond length. The optimized length is found to be 1.877 Å. (b) The optimization of bond angle. The optimized bond angle is found to be 118.57 degree.

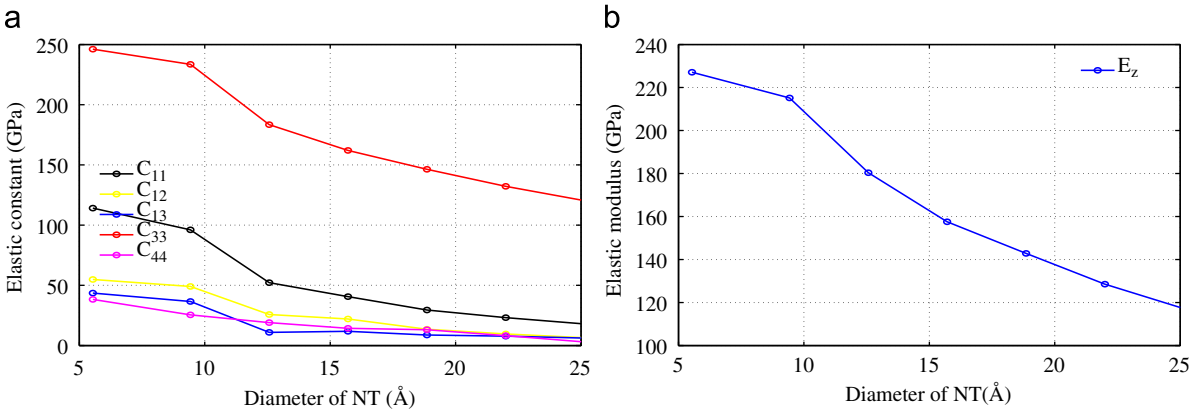

Fig. 3. Elastic properties of ZnO NTs as a function of tube diameter (Å). The elastic tensor components and axial Young's modulus are decreasing monotonically with increase in tube diameter. (a) Elastic constants of ZnO NTs. (b) Axial Young's modulus of ZnO NTs.

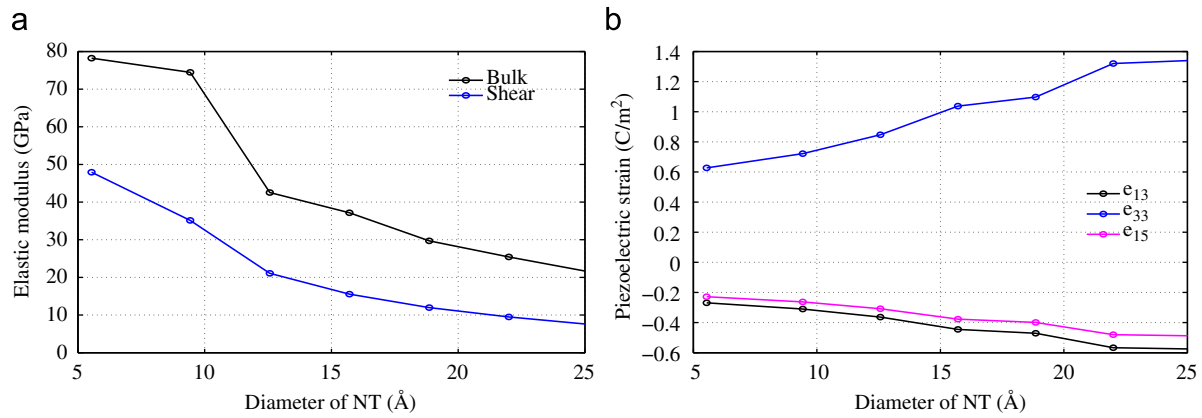

Fig. 4. Bulk material properties and piezoelectric strain coefficients of ZnO NTs as a function of tube diameter (Å). A strong increase of the piezoelectric constant e_{33}, which is supported by other studies for nanowires [54]. The absolute value of the effective piezoelectric constant e_{31} also increases with increasing NTs diameter, but the value is approximately half of the corresponding e_{33}, supported by other studies [55]. (a) Bulk and shear moduli of ZnO NTs. (b) Piezoelectric strain components of ZnO NTs.

the possibility of synthesizing single-walled ZnO nanotubes [50]. The geometry optimizations were performed with nanotubes rolled up from a graphitic ZnO single layer. The optimized bond length of Zn–O is found to be 1.877 Å [51], which is shorter than the bond length of 1.992 Å in wurtzite ZnO crystal. The average bond angle of ∠ Zn–O–Zn and ∠ O–Zn–O of the optimized tube is found 118.57. The variation of bond length and bond angle, of a typical ZnO nanotube, during the optimization process is shown in Fig. 2. The periodic boundary condition is applied in the axial direction.

5. Properties of ZnO nanotubes

Carbon nanotubes [52] are perhaps the most studied nanotube structures. Unlike the carbon nanotube, the synthesized ZnO nanotube [53] not only has a periodic structure along its axial direction, but also characterizes the feature of a finite crystal [12,17], which is the so-called single crystal nanotube. The ZnO NTs considered are also fully relaxed. The elastic constants as well Young's moduli of these ZnO NTs are calculated; they are plotted in Fig. 3. The elastic tensor components are useful to estimate the Poisson's ratio using the formula given in [54]. From Fig. 3, we can observe several aspects exhibited in the curves: (1) the values of the elastic constants decrease monotonically with the increase in the tube diameter; (2) the values of Young's moduli decreases as the tube diameter increases; and (3) Young's moduli values of the tubes exhibit higher than the single crystal (163.51 GPa) for $D \leq 14$ Å. However, bulk and shear moduli values Fig. 4(a) of the tubes exhibit lower value than single crystal (119.34 GPa). The variation of piezoelectric properties are presented in Fig. 4(b). We observe a strong increase of the piezoelectric constant e_{33} with the increasing diameter, which is supported by other studies for nanowires [54]. The absolute value of the effective piezoelectric constant e_{31} also increases with increasing NTs diameter, but the value is approximately half of the corresponding e_{33}, supported by other studies [55].

6. Conclusions

The elasticity and piezoelectric properties of single crystalline ZnO nanotubes are investigated using molecular simulations. A Buckingham type interatomic potential has been used for numerical calculations. Good agreements have been achieved between the present results and available results in the literature for wurtzite ZnO. Complete information of the elements of elastic tensors are necessary to derive other mechanical properties (e.g., Young's moduli, shear moduli, etc.). Therefore, the objective of the present study is to provide complete information about elastic and piezoelectric tensors of ZnO nanotubes. The elastic properties of ZnO nanotubes decreases with the increase in nanotubes diameters. The piezoelectric property of ZnO NTs is found to be also dependent on tube diameter. The effective piezoelectric constant e_{33} increases monotonically with the increasing diameter of the nanotubes. The absolute value of the effective piezoelectric constant e_{31} also increases with the increasing NTs diameter, and the value is around half of the corresponding e_{33}. The results derived in the paper can be useful for the design analysis of nano electromechanical devices involving ZnO nanotubes. The elastic and piezoelectric properties of ZnO nanotubes can be used as equivalent properties for simplified computational approaches, such as continuum models for ZnO nanotubes.

Acknowledgements

RC acknowledges the support of Royal Society through the award of Newton International Fellowship. SA gratefully acknowledges the support of The Leverhulme Trust for the award of the Philip Leverhulme Prize.

References

[1] U. Ozgur, Y. Alivov, C. Liu, A. Teke, M. Reshchikov, S. Dogan, V. Avrutin, S. Cho, H. Morkoc, Journal of Applied Physics 98 (2005).
[2] Z.C. Tu, X. Hu, Physical Review B 74 (2006).
[3] M. Catti, Y. Noel, R. Dovesi, Journal of Physics and Chemistry of Solids 64 (2003) 2183.
[4] D. Look, D. Reynolds, J. Sizelove, R. Jones, C. Litton, G. Cantwell, W. Harsch, Solid State Communications 105 (1998) 399.
[5] R. Khanna, K. Ip, Y. Heo, D. Norton, S. Pearton, F. Ren, Applied Physics Letters 85 (2004) 3468.
[6] Q. Wan, Z. Xiong, J. Dai, J. Rao, F. Jiang, Optical Materials 30 (2008) 817.
[7] Y. Yu-Rong, Y. Xiao-Hong, G. Zhao-Hui, D. Yu-Xiang, Chinese Physics B 17 (2008) 3433.
[8] F. Decremps, F. Datchi, A. Saitta, A. Polian, S. Pascarelli, A. Di Cicco, J. Itie, F. Baudelet, Physical Review B 68 (2003).
[9] Z. Tang, G. Wong, P. Yu, M. Kawasaki, A. Ohtomo, H. Koinuma, Y. Segawa, Applied Physics Letters 72 (1998) 3270.
[10] J. Huepkes, B. Rech, O. Kluth, T. Repmann, B. Zwaygardt, J. Mueller, R. Drese, M. Wuttig, Solar Energy Materials and Solar Cells 90 (2006) 3054.
[11] Z. Wang, Journal of Physics-Condensed Matter 16 (2004) R829.
[12] J. Hu, X.W. Liu, B.C. Pan, Nanotechnology 19 (2008).
[13] Y. Qin, X. Wang, Z.L. Wang, Nature 457 (2009) 340.
[14] T. Thundat, Nature Nanotechnology 3 (2008) 133.
[15] E. Gerstner, Nature Physics 4 (2008) 166.
[16] S. Xu, Y. Wei, J. Liu, R. Yang, Z.L. Wang, Nano Letters 8 (2008) 4027.

[17] S.L. Mensah, V.K. Kayastha, I.N. Ivanov, D.B. Geohegan, Y.K. Yap, Applied Physics Letters 90 (2007).
[18] Z.L. Wang, Applied Physics A—Materials Science & Processing 88 (2007).
[19] F. Claeyssens, C. Freeman, N. Allan, Y. Sun, M. Ashfold, J. Harding, Journal of Materials Chemistry 15 (2005) 139.
[20] X.J. Liu, J.W. Li, Z.F. Zhou, L.W. Yang, Z.S. Ma, G.F. Xie, Y. Pan, C.Q. Sun, Applied Physics Letters 94 (2009).
[21] W.F. Perger, J. Criswell, B. Civalleri, R. Dovesi, Computer Physics Communications 180 (2009) 1753.
[22] J. Qi, D. Shi, B. Wang, Computational Materials Science 46 (2009) 303.
[23] H. Ni, X. Li, Nanotechnology 17 (2006) 3591.
[24] M. Arnold, P. Avouris, Z. Pan, Z. Wang, Journal of Physical Chemistry B 107 (2003) 659.
[25] R. Zhu, D. Wang, S. Xiang, Z. Zhou, X. Ye, Sensors and Actuators A—Physical 154 (2009) 224.
[26] A. Asthana, K. Momeni, A. Prasad, Y.K. Yap, R.S. Yassar, Applied Physics Letters 95 (2009).
[27] R. Agrawal, H.D. Espinosa, Journal of Engineering Materials and Technology—Transactions of the ASME 131 (2009).
[28] A.V. Desai, M.A. Haque, Sensors and Actuators A—Physical 134 (2007) 169.
[29] M. Riaz, O. Nur, M. Willander, P. Klason, Applied Physics Letters 92 (2008).
[30] M. Lucas, W. Mai, R. Yang, Z.L. Wang, E. Riedo, Nano Letters 7 (2007) 1314.
[31] W. Mai, Z.L. Wang, Applied Physics Letters 89 (2006).
[32] C. Chen, Y. Shi, Y. Zhang, J. Zhu, Y. Yan, Physical Review Letters 96 (2006).
[33] A. Kulkarni, M. Zhou, F. Ke, Nanotechnology 16 (2005) 2749.
[34] A.J. Kulkarni, M. Zhou, Acta Mechanica Sinica 22 (2006) 217.
[35] G. Paglia, A. Rohl, C. Buckley, J. Gale, Journal of Material Chemistry 11 (2001) 3310.
[36] A. Brodka, P. Sliwinski, Journal of Chemical Physics 120 (2004) 5518.
[37] A. Brodka, A. Grzybowski, Journal of Chemical Physics 117 (2002) 8208.
[38] J.F. Nye, Physical Properties of Crystals, Clarendon Press, Oxford, 1985.
[39] E.R. Cope, M.T. Dove, Journal of Applied Crystallography 40 (2007) 589.
[40] J. Gale, A. Rohl, Molecular Simulation 29 (2003) 291.
[41] J.J. Gilman, Electronic Basis of the Strength of Materials, Cambridge University Press, Cambridge, UK, 2003.
[42] H. Karzel, W. Potzel, M. Kofferlein, W. Schiessl, M. Steiner, U. Hiller, G. Kalvius, D. Mitchell, T. Das, P. Blaha, et al., Physical Review B 53 (1996) 11425.
[43] X. Wu, D. Vanderbilt, D. Hamann, Physical Review B 72 (2005).
[44] E. Kisi, M. Elcombe, Acta Crystallographica Section C—Crystal Structure Communications 45 (1989) 1867.
[45] I. Kobiakov, Solid State Communications 35 (1980) 305.
[46] T. Azuhata, M. Takesada, T. Yagi, A. Shikanai, S. Chichibu, K. Torii, A. Nakamura, T. Sota, G. Cantwell, D. Eason, et al., Journal of Applied Physics 94 (2003) 968.
[47] H. Xu, R.Q. Zhang, X. Zhang, A.L. Rosa, T. Frauenheim, Nanotechnology 18 (2007).
[48] Y. Xing, Z. Xi, X. Zhang, J. Song, R. Wang, J. Xu, Z. Xue, D. Yu, Solid State Communications 129 (2004) 671.
[49] A. Wei, X. Sun, C. Xu, Z. Dong, M. Yu, W. Huang, Applied Physics Letters 88 (2006).
[50] Z. Fu-Chun, Z. Zhi-Yong, Z. Wei-Hu, Y. Jun-Feng, Y. Jiang-Ni, Chinese Physics Letters 26 (2009).
[51] B. Wang, S. Nagase, J. Zhao, G. Wang, Nanotechnology 18 (2007).
[52] S. Iijima, Nature 363 (1993) 603.
[53] G. Patzke, F. Krumeich, R. Nesper, Angewandte Chemie International Edition 41 (2002) 2446.
[54] A. Mitrushchenkov, R. Linguerri, G. Chambaud, Journal of Physical Chemistry C 113 (2009) 6883.
[55] Y. Xi, J. Song, S. Xu, R. Yang, Z. Gao, C. Hu, Z. Wang, Journal of Materials Chemistry 19 (2009) 9260.